GEOFIZIKA VOL. 13 1996

Original scientific paper
UDC 551.511.61

Numerical simulations of dissipation of dry temperature inversions in basins

Tomaž Vrhovec and Andrej Hrabar

University of Ljubljana, Department of Physics Ljubljana, Slovenia

Received 25 June 1996, in final form 20 October 1996

A hydrostatic mesometeorological model APIKA (Vrhovec, 1991) was improved by a new turbulence parametrisation using a complete prognostic equation for the turbulent kinetic energy with both horizontal and vertical advection of turbulent kinetic energy. Horizontal diffusion of momentum and heath by turbulence is explicitly included.

Three different forcings of temperature inversion layer dissipation in basins were studied: dissipation due to diabatic (thermal) forcing, dissipation due to the advection of colder air and dissipation due to wind shear. We show that in winter time the dissipation due to the cold air advection and dissipation due to increasing wind speed aloft are efficient enough to cause mixing of deep cold air lakes while irradiation thermal forcing at 45 °N in deep basins is often insufficient to dissipate the inversion in deep basins when ground is cowered with snow.

Keywords: Numerical simulation, dry temperature inversion

Numeričke simulacije disipacije temperaturnih inverzija u kotlinama

Hidrostatski mezometeorološki model APIKA (Vrhovec, 1991) nedavno je dopunjen novom shemom parametrizacije turbulencije uporabom kompletne prognostičke jednadžbe za turbulentnu kinetičku energiju s horizontalnom i vertikalnom advekcijom turbulentne kinetičke energije. Horizontalna difuzija zbog turbulencije je eksplicitno dodana u jednadžbe gibanja.

Razmotrena su tri različita mehanizma disipacije temperaturnih inverzija: pomoću modela disipacije zbog dijabatskog (termičkog) forsiranja, zbog advekcije hladnog zraka i zbog vertikalnog gradijenta vjetra. Forsiranje zbog advekcije hladnijeg zraka i zbog verikalnog gradienta vjetra zimi je dovoljno snažno da uzrokuje disipaciju inverzije u dubokim kotlinama. Forsiranje zbog sunčane iradijacije zimi često ne može disipirati inverziju ako je reljef prekriven snijegom.

1. Introduction

In the absence of strong synoptic scale flow above a complex topography the fair weather local winds are mostly forced by the differences in local diabatic heating or cooling. In daytime the differences in diabatic heating are due to the diverse inclination and aspects of the slopes. The intensity of local heating of the atmosphere is further modified by the differences in local surface reflexivity and in heat storage.

During the night and in the absence of clouds, the forcing term in the energy balance of surface of the topography is IR terrestrial radiation. As in anticyclonic weather with synoptic scale subsidence the clouds are usually absent, it is justified to assume that the incoming IR atmospheric radiation is horizontally homogenous (assuming also that water vapour content is homogeneous in the atmosphere). The net IR radiation at the terrain surface at night is then modified by the differences in topography, the ground parameters and in the ground emissivity only.

The nocturnal diabatic forcing of the winds in basins and in valleys is more or less the same, but final temperature and wind fields are dissimilar. Due to diverse geometry of a basin (a basin has no or only a small outflow, Petkovšek, 1978), the basin winds are more confined into the basin and its surroundings, while the valley wind system affects also the tributary valleys and nearby plains (for review see Whiteman, 1990). In the night the cold air formed along the slopes and at the bottom of a basin can not flow out of it as it does out of the valley creating downvalley wind. The cold air simply accumulates in the basin: the upper boundary of cold air can be seen as a rising elevated temperature inversion layer. The morning transition of wind and temperature stratification is in basins again different than in the valleys: due to stronger inversion layer (Petkovšek, 1992), it takes stronger forcing than in the valley for the air in the basin to mix (or it also takes longer for the basin atmosphere to mix). As the inflow from surroundings into the basin is limited, (as well as the outflow during the night) winds are mostly recirculating within the basin atmosphere.

In this paper we will present some results of the simulations of dissipation of temperature inversion layers (for non saturated cases) within basins. The dissipation of the inversions was modelled with three different forcings:

a) thermal dissipation with a complete parametrisation of turbulence by turbulent kinetic energy equation,

b) dissipation by colder air advection aloft,

c) dissipation by wind shear aloft the inversion.

The three forcings are the usual reasons for dissipation of inversion layers. The thermal dissipation is the most usual one in the warmer part of the year and our aim was to verify if the thermal forcing alone can dissipate the inversion layer in deep basins also in winter when the ground is snow covered.

The second aim was to determine the time needed for turbulent wind shear dissipation of inversions. In winter time and in cloudy weather when thermal dissipation of inversions is suppressed, the turbulent wind shear dissipation is in absence of frontal disturbances the only possible way for the air below and above inversion to mix. The time needed for the dissipation of inversion layers in basins can be of great practical importance, since the limited volume of air below the inversion can be polluted rapidly even by moderate emissions. The decisions concerning limiting of emissions (traffic, power plants, heating) must be made knowing what the development of inversion layer will be in the next hours, in order to keep concentrations of pollutants below critical levels.

2. Model description

The simulations of dissipation were performed with an improved version of the mesometeorological model APIKA (Vrhovec, 1991). The model APIKA is a three dimensional, fine mesh, limited area, mesoscale, dynamical, anelastic, Boussinesq model with hydrostatic limitations using complete prognostic three dimensional equations for horizontal wind velocities u and v, prognostic equation for potential temperature θ, diagnostic continuity equation for vertical velocity w and hydrostatic equation for Exner function π as described by Pielke (1984). It was designed to resolve processes in a very steep topography and it showed good performance in various cases of wind adjustment to the topography obstacles (blocking of the flow) (Vrhovec, 1991; Vrhovec et al., 1992). The topography is represented by blocks and the mesh is three times staggered (Arakawa C grid, Mesinger and Arakawa, 1976). As model uses block topography and model space calculation levels are horizontal, the vertical velocities and vertical accelerations are reduced in comparison to models that use terrain-following co-ordinates. As vertical accelerations are small the hydrostatic approximation can be used also with steep topography gradients. In horizontal direction model space resolution is 3 km (if not stated otherwise by particular simulation). Vertical model space resolution varies with height: in lower part of model atmosphere (up to the upper boundary of inversion layer) the vertical spacing is from 10 to 50 meters; higher the spacing is from 100 to 400 meters.

To determine net diabatic effects the model uses radiation scheme similar to the ones used by Pielke (1984) and finally determines diabatic substantial changes of potential temperature with a help of energy balance equation. For the determination of the soil/snow surface temperature the model uses prognostic equation for soil temperature profile. Snow is introduced as the uppermost layer of soil with reduced conductivity and high albedo. The model atmosphere is initialised by a single vertical temperature and wind profile. Before diabatic effects are introduced, the model is run in adiabatic turbulent mode to enable adjustment of wind field to the topography.

Model APIKA uses a second order closure turbulence scheme. To determine turbulent diffusivities for the momentum and for the heat in all three dimensions parametrisation using turbulent kinetic energy (TKE) was employed.

Turbulent diffusivity for the momentum in vertical direction (K_{mv}) is determined by (Pielke, 1984):

$$K_{mv} = l_m(aE)^{0.5} \tag{1}$$

where l_m, is characteristic turbulent length scale. E is TKE.

The TKE is transported, created by shear and buoyancy, dissipated and turbulently mixed:

$$\frac{\partial E}{\partial t} = -u\frac{\partial E}{\partial x} - v\frac{\partial E}{\partial y} + w\frac{\partial E}{\partial z} + K_{mv}\left[\left(\frac{\partial u}{\partial z}\right)^2 + \left(\frac{\partial v}{\partial z}\right)^2\right] - K_{hv}\frac{g}{\theta}\frac{\partial \theta}{\partial z} -$$

$$-\frac{c_E}{l\,E^{1.5}} + \frac{\partial K_{mh}\,(\partial E/\partial x)}{\partial x} + \sigma_E\frac{\partial K_{mh}\,(\partial E/\partial z)}{\partial z} \tag{2}$$

The parameters a, c_E and σ_E are determined as in Bischoff-Gauss (1982) or Deardroff (1980), while vertical turbulent diffusivities for enthalpy K_{hv} and for momentum K_{mv} and horizontal diffusion for momentum K_{mh} are determined according to Deardroff (1980).

The advection terms are evaluated by forward upstream scheme while others are determined by central differences. The turbulent kinetic energy equation (2) is integrated in time by the iterative Heun scheme. The time step is variable and is adjusted in each time step to the advection velocity and the CFL criterion. The initial state of turbulent kinetic energy is determined as a fraction of energy and so also for turbulent diffusivity. The minimum requirement for turbulent diffusivity acts as an implicit numeric filter in numerical integration of momentum and enthalpy equations of the model.

In the comparison to the lower order closure with the length l_m that is completely diagnostic and local, the turbulent kinetic energy approach enables also the transport of turbulence from the regions of more perturbed flow into less perturbed surroundings. This effect is important in the case of a basin on a plateau as the turbulent flow from the plateau is still turbulent as it moves upon the stagnant air in the basin or valley.

3. Diabatically forced dissipation: DIBAJA case

DIBAJA case simulates the atmosphere above a deep basin in January, when topography is snow-covered. The basin's flat bottom which is 5 km long and 4 km wide is 300 m lower than the surrounding plateau. The maximum

inclination of the slopes is 37° (75%). We choose such a topography to get solar irradiation almost perpendicular to the south facing slopes approximately at solar noon in mid January at about 45 °N. The model stays within hydrostatic limitations as maximum vertical velocities in this simulation are much less than 1 m/s and maximum vertical accelerations are 0.015 m/s^2.

For this special case the model space has horizontal resolution of 1 km and 18 levels in vertical direction in the air and 10 levels in the snow and the ground. It is assumed that the whole basin and the plateau have the same short wave albedo (0.9). In the DIBAJA case there is no initial wind. The results of this simulation are presented with a set of figures of vertical cross-sections of the temperature along basin's longer axis and vertical temperature profiles for a point in the middle of the basin.

In the DIBAJA case the simulation started with moderately stable temperature stratification (uniform vertical temperature gradient of –0.6 K/100 m) at 1:00 LT (local time) and after three and half hours of simulation (more than 3:30 h before the sunrise) basin is almost full of cold air. The model atmosphere is divided into three layers: the basin atmosphere (about 200 m deep, with the average vertical temperature gradient of –0.7 K/l00 m), the inversion layer (about 150 m deep, with the vertical temperature gradient of +0.6 K/l00 m) and the »free« atmosphere above 600 meters with the vertical temperature gradient of –0.8 K/100 m. In the next three hours (local sunrise is at 8:00 LT, Fig. 1) the temperature field in the basin hardly changes: there

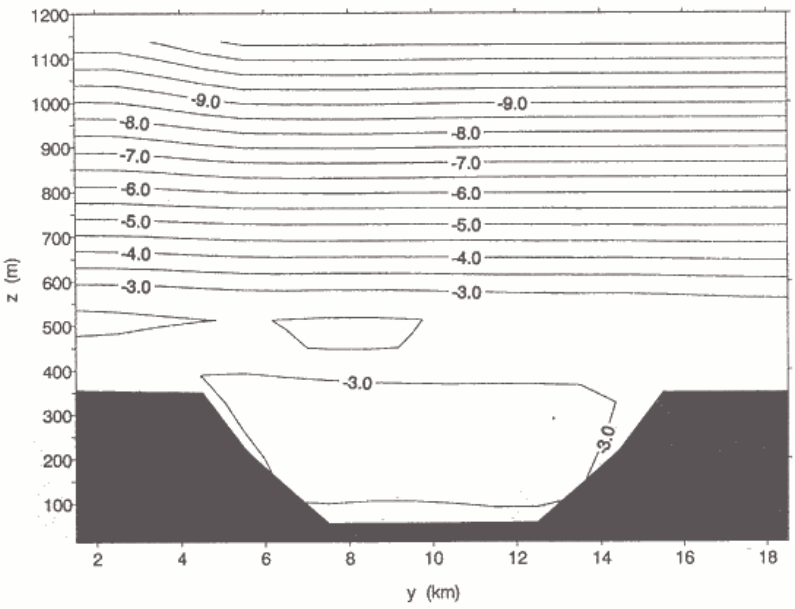

Figure 1. DIBAJA case: temperature (in °C) cross-section along the longer basin axis in a deep basin just after sunrise (8:28 LT, 7:28 h after beginning of simulation, for a January day). South-facing slope is at the right side of the figure.

is ground inversion layer also above the surrounding plateau, the winds that were still circulating during the formation of elevated inversion within basin atmosphere decrease – at the time of sunrise there is almost no wind.

As the ground is covered with snow with high albedo and low conductivity there is only small diabatic heating of the air from the ground after sunrise and the inversion layer persists for the whole morning. There are no winds within the basin atmosphere. One hour after the local noon the inversion layer begins partly to dissipate on the south facing slope of the basin. At first there is some updraft there, the temperature stratification becomes less stable, but at the north facing slope the inversion persists (Fig. 2). The main part of the basin atmosphere has almost isothermal stable stratification (Fig. 4). Later in the afternoon the radiation energy impacting the south facing slopes decreases rapidly suppressing also the dissipation process, and the atmosphere near the slopes starts to cool again. Just after the sunset (Fig. 3) the inversion layer across the whole basin at the height of basin the rim is re-established. Near the slopes the air starts to cool and again there is descending motion along the slopes – the basin is being refilled with the cold air. The vertical temperature stratification for a point in the middle of the model atmosphere is depicted at Fig. 4 for the same times as for the vertical cross-sections. There are only slight changes in the basin during the morning (temperature increases for 0.5 K). In the afternoon, as the incoming sun radiation decreases, there is cooling of about 1 K at the height near the basin rim.

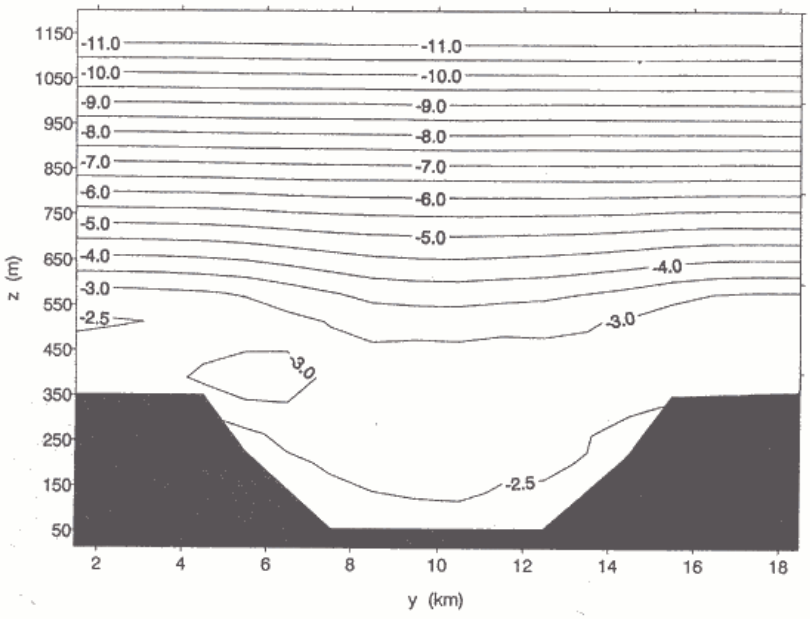

Figure 2. DIBAJA case: temperature cross-section along the longer basin axis in a deep basin as inversion begins partly to dissipate (14:04 LT, 13:04 h after beginning of simulation, for a January day). South-facing slope is at the right side of the figure.

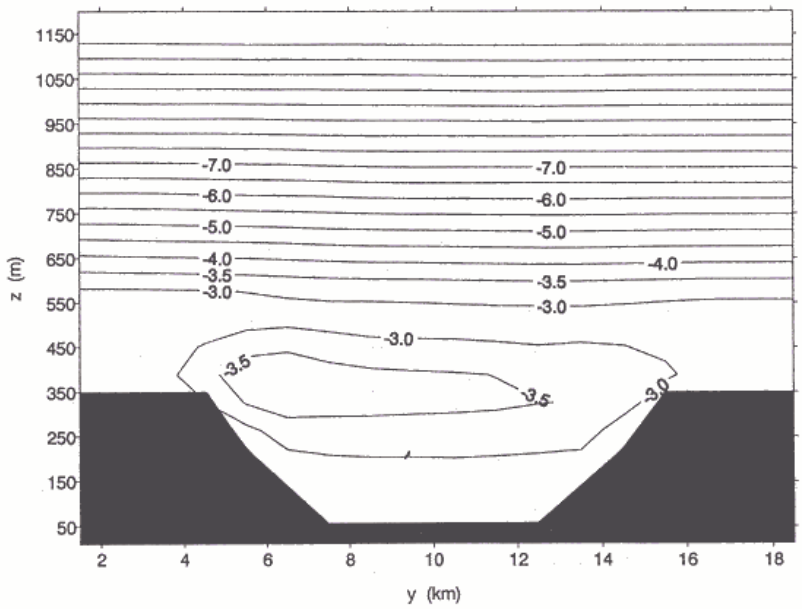

Figure 3. DIBAJA case: temperature cross-section along the longer basin axis in a deep basin after sunset, (17:22 LT,16:22 h after beginning of simulation, for a January day).

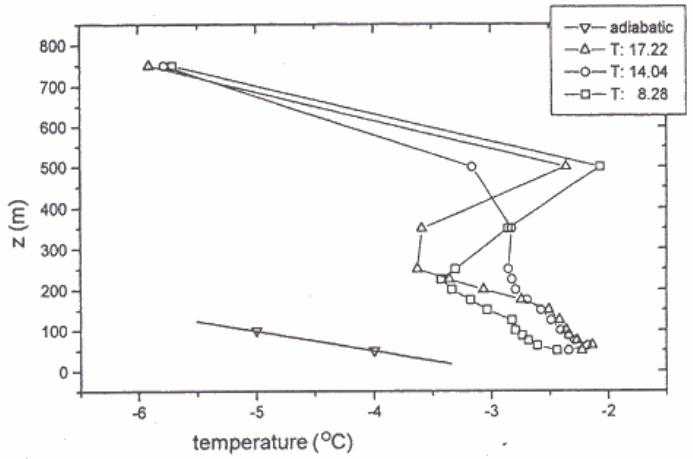

Figure 4. DIBAJA case: vertical temperature profiles for a point in the middle of the basin at various times after beginning of simulation.

The DIBAJA case shows that in winter, while ground is snow-covered, even at clear skies the incoming solar energy is not strong enough to dissipate the inversion layer in a deep basin. The dissipation just starts at the south facing slopes but the whole basin atmosphere is only little affected by it. The air that was stagnant in the lower part of the basin atmosphere stays there and the winds are just mixing the air within the basin.

To determine a more general relationship between the energy balance and possible dissipation of the elevated inversion over a basin we calculated the cumulative energy balances for the dry inversion layers. As incoming solar

radiation is in fact the only net input of the energy into the atmosphere/soil system we assumed that just a fraction (it is determined by the surface albedo and emisivity) of incoming solar energy is converted into sensible heat that causes the inversion layer heating and subsequently its dissipation. For inversion layer of 5 K elevated 200 m above the basin bottom it is necessary to supply about 280 Wh/m^2 for the inversion to dissipate (Hočevar et al., 1982). On the plots in Fig. 5 we depicted the cumulative energy for three different days (March, June and December) for clear and cloudy sky. For a cloudy day the incoming insolation is reduced due to the albedo of the clouds. It is evident that even on a clear day in winter the available energy is almost always too small to dissipate the cold air layer in the basin. If the sky is cloudy in summer, such a layer can be dissipated by the sun radiation only. With the DIBAJA case we showed that on the south-facing slopes the inversion layer can be partially dispersed but only in case of almost perpendicular irradiation. The combination of a high albedo, low thermal conductivity of snow cover and high IR emisivity maintains the inversion on all other places in topography throughout the day.

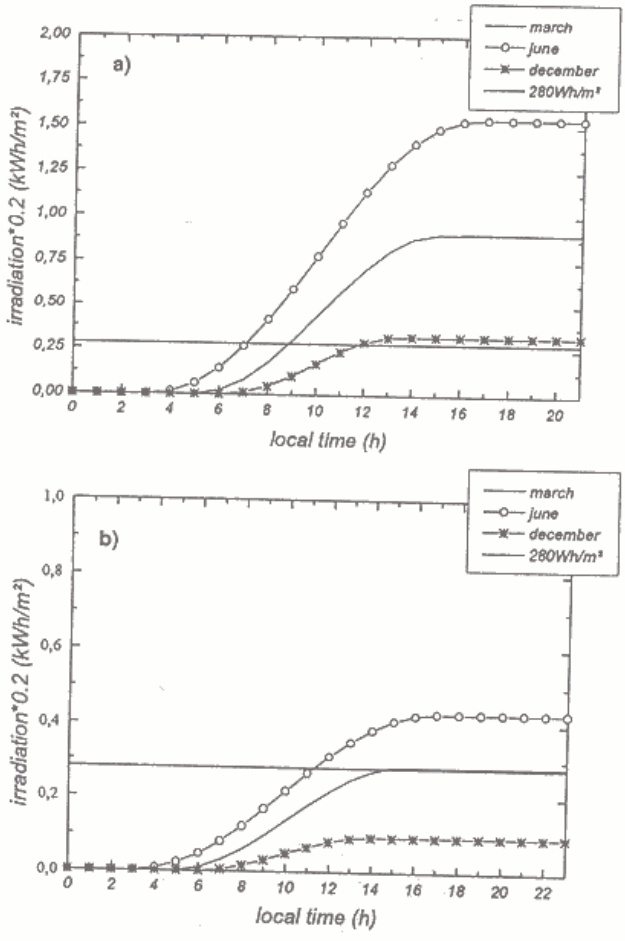

Figure 5. Cumulative net available energy (solar irradiation transformed into sensible heat, with surface albedo of 0.2) for three days. a) for clear skies, b) for cloudy skies.

4. Simulation results of dynamically forced dissipations

4.1. Cold air advection in the basin – CAADBA case

To study the dissipation of elevated dry (non-saturated) temperature inversion by cold air advection we used a simplified version of the APIKA model. In this case most of the diabatic forcing was excluded and turbulent mixing was reduced (Hrabar, 1995). Initially there was already an inversion layer in the model atmosphere and the air is stagnant. To simulate the advection of cold air from the exterior of the model space (like an approaching cold front) some modifications of model boundary conditions were made. One of the lateral boundaries of the model space was gradually cooled in time and starting from topography surface up, with the rate corresponding to the inclination of a cold front (inclination 1/100). As some of the characteristics of cold front were not modelled at the boundary (like the tangential flow), the front evolved by itself in the model space. The invading cold air was initially stagnant and there was infinite supply of the incoming air. The advection velocity was generated by pressure differences due to cooling only, and the cold front accelerated as a gravity current. The cold front gravity current was moving with a maximum speed of 6 m/s while still above the horizontal plateau, before reaching the basin depression. When the cold air reached the slopes its horizontal velocity increased up to 10 m/s and the vertical one up to 0.3 m/s. As the gravity current was not in a geostrophic balance (the gravity current wind was initially blowing in the direction of the temperature and pressure gradients), some geostrophic adjustment was observed and wind got also a component tangential to the cold front surface. The invading cold air is moving along the topography and the warmer air aloft is displaced horizontally and vertically. Horizontal and vertical velocities and accelerations are higher in the CAADBA case than in the DIBAJA case, so we had to reduce the maximum topography gradients to stay within the hydrostatic limitations. The shape of the model topography is changed just by changing the horizontal grid from 1 km in the DIBAJA case to 3 km in the CAADBA case.

Initially the invading cold air was 4 K cooler than the model atmosphere at the same heights and there was a 3 K inversion layer 50 meters thick (vertical temperature gradient 0.06 K/m) at the height of the upper basin rim. Here we present some results (temperature cross-sections) along the longer axis of the basin and the time evolution of the vertical temperature profile.

As the cold front approaches the basin, the temperature difference between the invading cold air and the model atmosphere causes the gravity current winds to develop. This wind advects the cold air and the invading air descents into the basin atmosphere. The cold air is potentially just slightly cooler then the basin air. It accelerated due to a descent into the basin and the front gradually moves across and into the basin. After two hours the invading air is near the upper rim (Fig. 6) and the initial inversion layer is

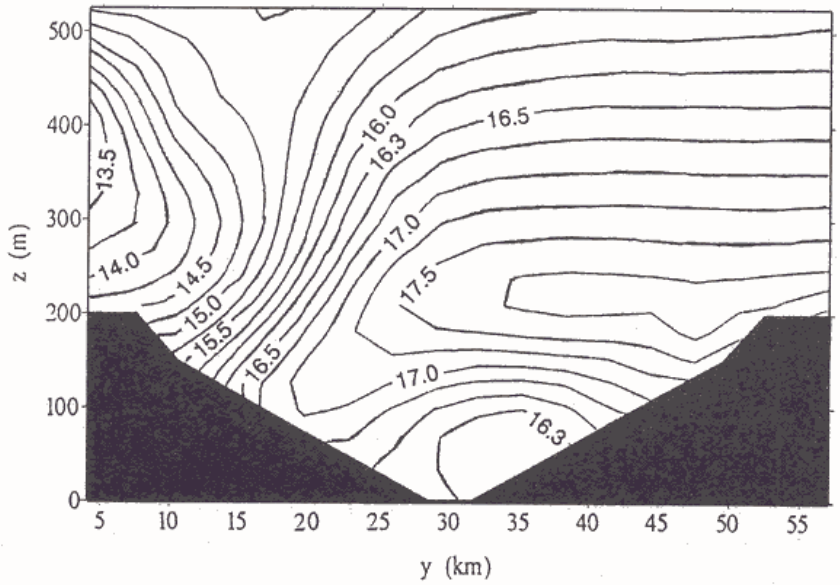

Figure 6. CAADBA case: temperature cross-section along the basin longer axis 2 h and 18 min after beginning of advection. Cold air begins descent into the basin.

still above most of the basin. As the basin air is forced to move out of the basin, it rises along the opposite slope (Fig.7) and cools adiabatically causing the inversion to get temporary stronger there. In the next hour the most of

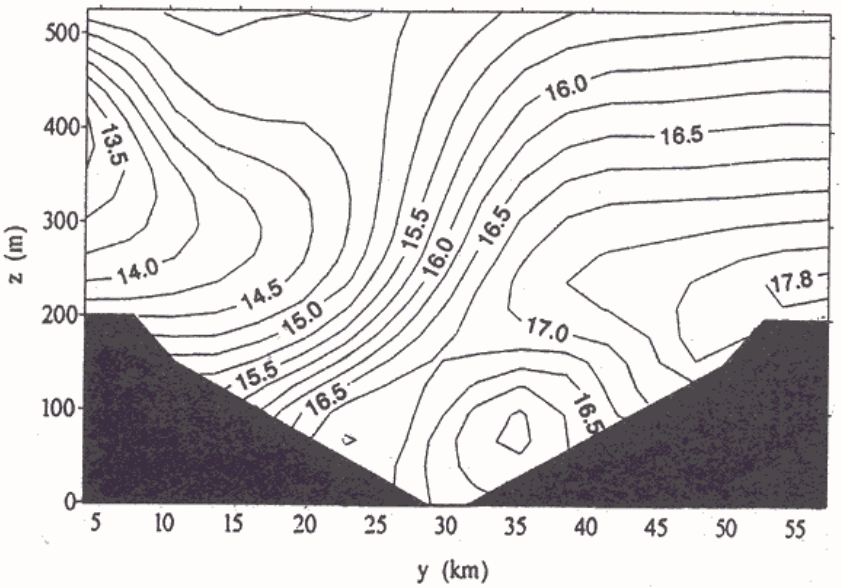

Figure 7. CAADBA case: temperature cross-section along the basin longer axis 2 h and 49 min after beginning of advection. Cold air from the basin is forced up the lee slope.

the basin air is forced out of the basin, the cold front air spreads over most of the model domain and less stable stratification is established (Fig. 8). The maximal wind velocities observed during the cold air advection were up to 10 m/s. The vertical temperature profiles for a point in the middle of the basin are shown in Fig. 9. For this point it took 3 h and 36 min from the beginning of the simulation or about 1 h and 20 min after the front reached the basin rim for the inversion to dissipate.

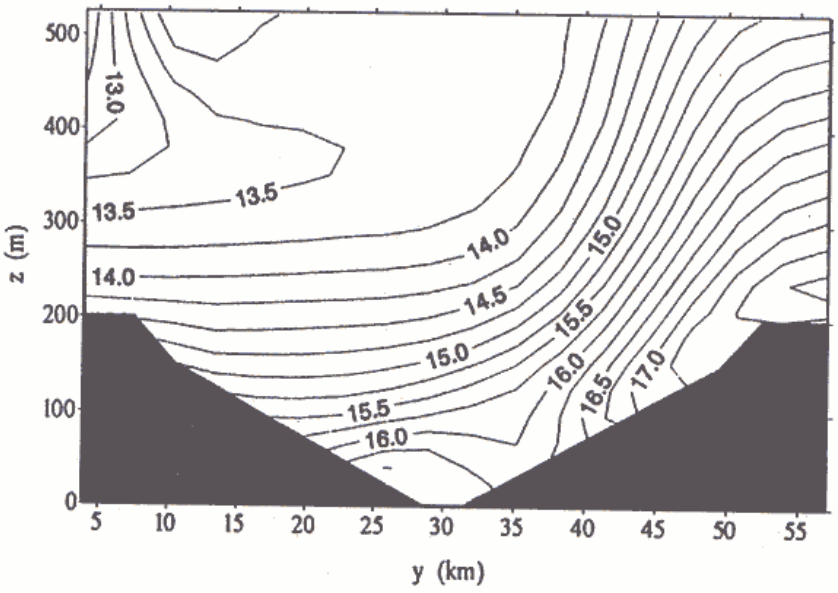

Figure 8. CAADBA case: temperature cross-section along the basin longer axis 3 h 36 min after beginning of advection. Normal stratification is established in most of the basin atmosphere.

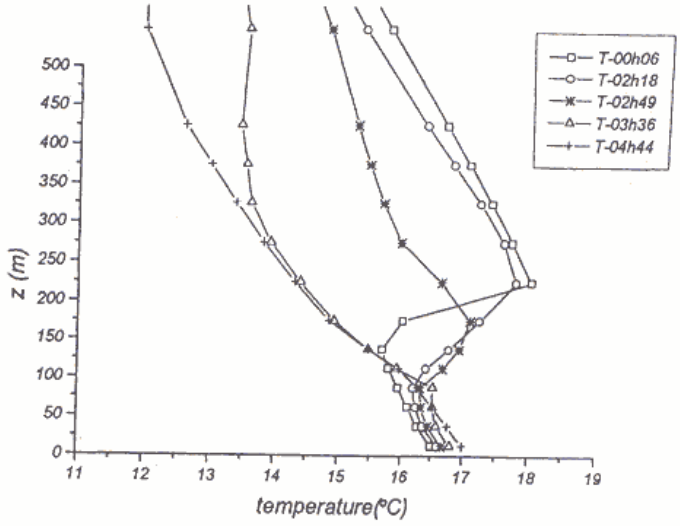

Figure 9. CAADBA case: vertical temperature profiles for a point in the middle of the basin at various times after beginning of simulation.

4.2 Turbulent dissipation of inversion layer in a basin: TUDIBA case

To simulate a turbulent dissipation of a dry inversion layer the model geometry was modified so that the model was running in a quasi two-dimensional version (the model space had just 5 points in the direction perpendicular to the flow direction). The shape of the basin is the same as in the CAADBA case. Additionally we increased the vertical resolution of the model space threefold. In this case we applied the complete turbulence parametrisation and included homogenous diabatic forcing. The atmosphere was assumed to be uniformly cloudy with just indirect solar irradiation (100 W/m^2). The initial geostrophic wind at the upper boundary of the model space (at 5500 m) was set to 5 m/s in this case. The wind field used for further simulation was obtained by 7 hours of adjustment of a geostrophically balanced flow to the topography. During this initial adjustment no inversion layer was present and the initial vertical temperature profile was the same as the initial profiles in the CAADBA and the DIBAJA cases (uniform vertical temperature gradient of –0.6 K/100 m). After the wind adjustment the initial state for the temperature was redefined by an elevated inversion layer between 150 and 200 meters above the basin bottom with the temperature difference of 3 K.

Two numerical experiments were performed. In the first case we tried to dissipate the inversion by a constant wind aloft. The wind at the model upper boundary was forced to have a constant velocity of 5 m/s during the time of simulation. In this case the inversion layer did not dissipate as shown in Fig. 10 – in fact the temperature difference even increased. The reason for non-dissipation is that TKE production at the upper boundary of the inversion layer was not sufficient. The calculation of the Richardson flux number gave

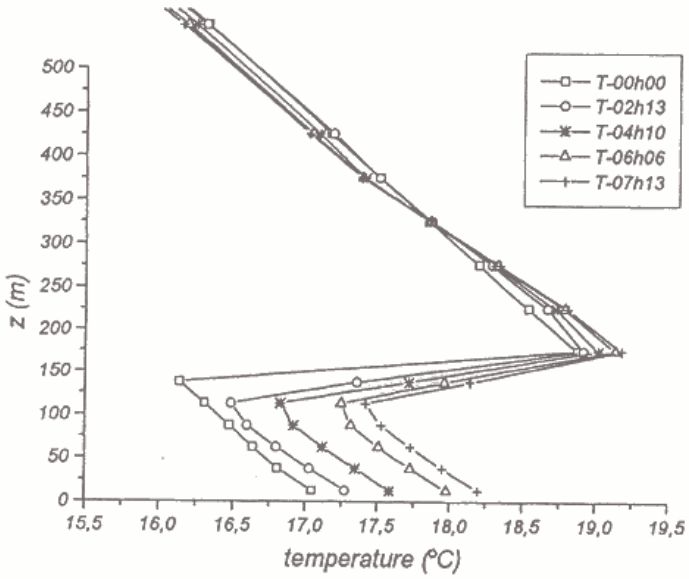

Figure 10. TUDIBA case: vertical temperature profiles for a point in the middle of the basin at various times after beginning of simulation, constant wind aloft. No dissipation.

results well within the region of a suppressed turbulence. The results of model simulation are well in accordance with the theoretical considerations (Petkovšek, 1992).

The second case was performed witha wind velocity increasing in time aloft the basin. With the same temperature stratification as before the inversion dissipated in approx. 11 h. The wind aloft was increasing for five hours from 5 m/s (in the first case of turbulent dissipation such a wind velocity did not enable dissipation of inversion layer) with the rate of (2.5 m/s)/h at the upper model boundary. We chose this increase rate as derived from theoretical considerations so that the TKE production was sufficient (Petkovšek, 1992). The pressure field at the upper boundary was all the time geostrophycally adjusted to increasing wind. Fig. 11 shows the changes of temperature stratification at the point in the middle of model domain. In this case it can also be seen that the temperature difference across the inversion increases in the first hours of dissipation but later the inversion height and temperature difference across the inversion layer decrease until the inversion layer dissipates. With increasing wind shear at the upper boundary of inversion layer the generating term in Eq. 2 increased, therefore also locally increasing the turbulent diffusivity. The time evolution of $\partial u/\partial z$ for a point at the middle of the basin is shown in Fig. 13. As the vertical gradient of wind velocity increases, the Richardson flux number decreases and the turbulence gets less suppressed (but the inversion layer is still present). The wind velocity is constantly increasing but the increase of $\partial u/\partial z$ is very pronounced between 2:20 and 4:10. That is also the moment when TKE production is great enough to start the dissipation process. As the invading air is warmer than the air under the inversion they mix gradually and the final temperature stratification is nearly neutral. Fig. 12 depicts the temperature cross-section along the

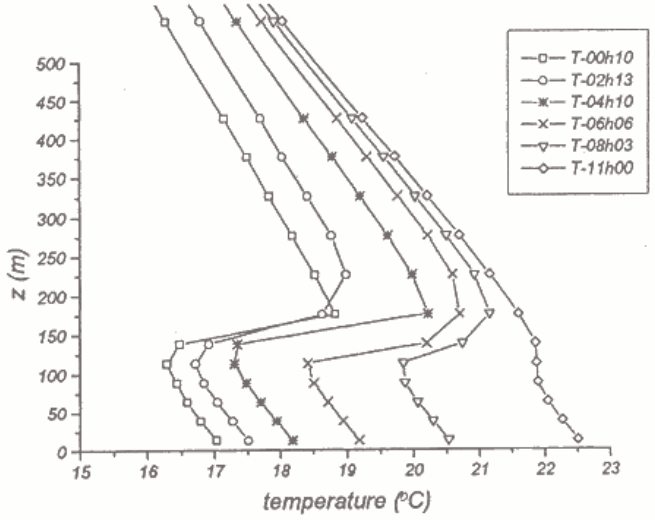

Figure 11. TUDIBA case: vertical temperature profiles for a point in the middle of the basin at various times after beginning of simulation, increasing wind. Dissipation of inversion layer.

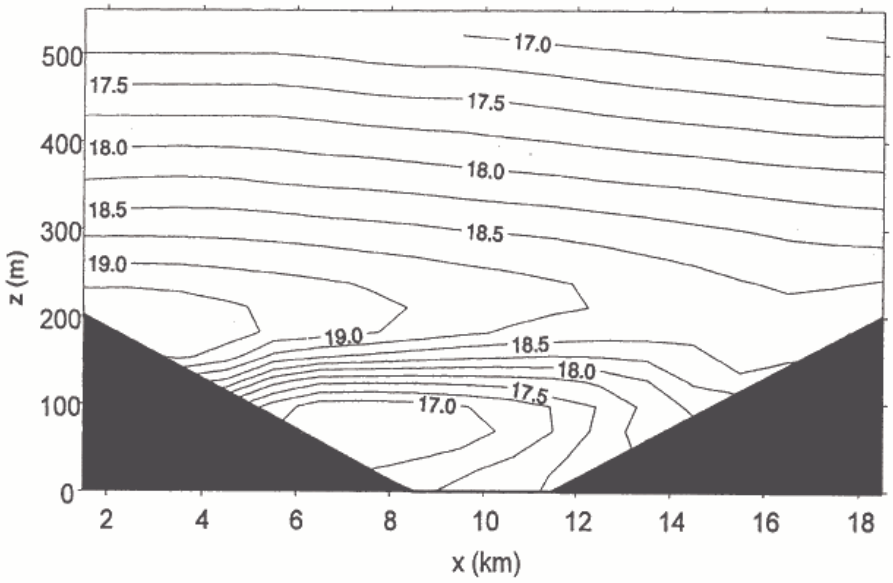

Figure 12. TUDIBA case: temperature cross-section along the basin longer axis 4 h and 10 min after beginning of advection. Turbulence starts do dissipate the inversion near the slopes.

basin longer axis, some hours (4:10) after start of the simulation and well before the inversion was completely dissipated. The formation of neutrally stratified atmosphere at the lee slope can be observed while there is still a strong inversion above most of the basin. During the dissipation of inversion layer some transient features like gravity waves are observed but they are effectively suppressed by a dissipative numerical advection scheme.

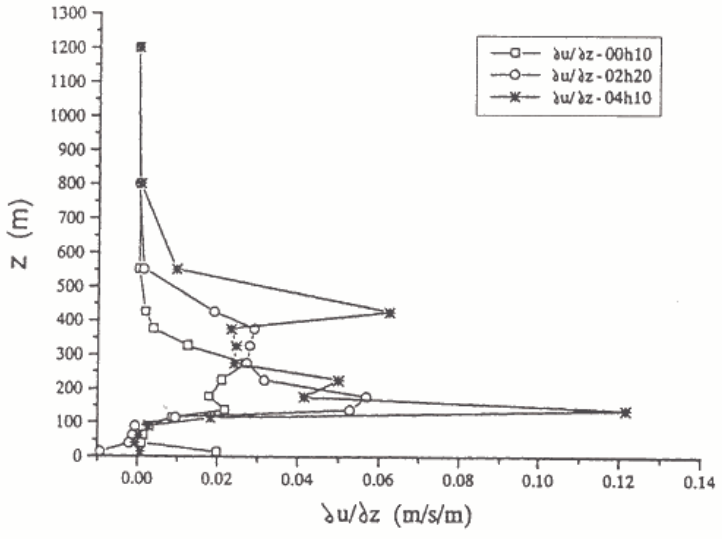

Figure 13. TUDIBA case: vertical profiles of $\partial u/\partial z$ for a point in the middle of the basin at various times after beginning of simulation, increasing wind aloft. Note the prominent peak at 200 m for the time 4:10.

5. Conclusions

According to our model simulation of different cases of dissipation of the dry (non-saturated) temperature inversions in a generic basin, the following can be stated:

– Diabatic (thermal, due to solar radiation) dissipation of dry temperature inversions is possible only in warmer half of the year. At times of low solar elevation the incoming solar radiation is not sufficient to heat the lower part of the atmosphere to enable the mixing of inversion layer with the exception of sun-facing slopes, where thermal dissipation can occur due to higher energy input and due to thinner layer of cold air. In deep basins the diurnal dissipation is impossible if the ground is snow-covered.

– Cold air advection is an effective way to dissipate dry temperature inversions in basins: it can remove the cold air resting in the basin rapidly also without any radiation forcing. It is not necessary for the advected cold air to be much cooler than the basin atmosphere, it is only necessary for the invading cold air to be potentially cooler than the air at the bottom of the basin.

– Turbulent dissipation of dry temperature inversion can occur if TKE production at the upper boundary of inversion is large enough. If wind velocity is constant, the inversion layer will not dissipate in case of moderate winds; if wind velocity is increasing it is possible to dissipate the inversion layer just by turbulence and without advection of colder air. The time for turbulent dissipation of temperature inversion layer can be long: our simulations show that with the wind velocity time rate of 2.5 m/s/h for 4 hours (starting with 5 m/s) the inversion can start to dissipate. It can take up to 11 hours for the turbulence to completely dissipate the cold air from the basin (Fig. 11). As often in colder part of the year the sunshine day is shorter, it is possible for diabatic cooling to start creating a new nocturnal inversion before the old one is completely dissipated. In the natural atmosphere the diabatic and the non-diabatic processes of the inversion layer dissipation are often present simultaneously: with the help of radiation forcing the times of inversion dissipation can be shortened, especially at the south-facing slopes.

The prediction of time for the dissipation of temperature inversion layers is an interesting problem in mesoscale forecasting and nowcasting especially in narrow valleys and basins in the colder part of the year. While the inversion layer persists and the temperatures in basins are much lower then in the surrounding atmosphere, there are often air pollution and traffic problems.

Assessing the way of dissipation and forecasting the time of dissipation can help making the decisions concerning air pollutants concentration limitation.

References

Bischoff-Gauss I. (1982): Zur Verwendung der Gleichung für Turbulenzenergie bei der Schliessung des Gleichungsystems für die atmosphaerische Grenzschicht, Diploma Thesis, Dept. Meteorol. Tech. Univ. Darmstadt. 45 pp.

Businger, J. A. *et al.* (1971): Relationships in the atmospheric surface layer. J. Atm. Sci., **28**, 181–189.

Deardroff, J. W. (1980): Stratocumulus capped mixed layers derived from a three dimensional model, Bound. Layer Meteor,**18**, 495–527.

Hočevar, A. *et al.* (1982): Solar irradiation in Slovenia: duration and energy, University Ljubljana, Slovenia, Biotechnical faculty, 96 pp.

Hrabar, A. (1995): Numerična simulacija nastanka in razkroja jezer hladnega zraka (Numerical simulation of cold air lake formation and dissipation), B. Sc. Thesis, FMF–Meteorology, University Ljubljana. 41 pp.

Mesinger, F. and A. Arakawa (1976): Numerical methods used in atmospheric models, GARP Pub. Ser. 17, WMO-ISCU, 64 pp.

Petkovšek, Z. (1978): Model for the evaluation of mean emission potential of the air pollution with $S0_2$ in basins. Archiv Met. Geoph. Biokl. B, **26**,199–206.

Petkovšek, Z. (1992): Turbulent dissipation of cold air lake in a basin. Meteorol. Atmos. Phys., **47**, 237–245.

Pielke R. A. (1984): Mesoscale meteorological modelling. Academic Press, Orlando, 612 pp.

Vrhovec, T. (1991): A cold air lake formation in a basin: a simulation with a mesoscale numerical model, Meteorol. Atmos. Phys., **46**, 91–99.

Vrhovec, T., N. Pristov, and A. Hočevar (1992): Theoretical and model assessment of air pollution deposition in an alpine headwater, Environmental regeneration in headwaters, Proœedings of the symposium, WASWC–IUFRO, Prague, 278–287.

Whiteman, C. D. (1990): Observations of thermally developed wind systems in mountainous terrain. Atmospheric processes over complex terrain. Am. metorol. Soc. Meteorological Monographs, 5–42.

Corresponding author's address: Dr. Tomaž Vrhovec, Chair for Meteorology, University Ljubljana, Department of Physics, Jadranska ul. 19, 1001 Ljubljana, Slovenia